

Supplementary Information

Materials and methods

Cell preparation. Machine made 220 mAh $\text{LiNi}_{1/3}\text{Mn}_{1/3}\text{Co}_{1/3}\text{O}_2$ /graphite (NMC/graphite) pouch cells were obtained dry (vacuum sealed with no electrolyte) from Li-Fun Technology (Xinma Industry Zone, Golden Dragon Road, Tianyuan District, Zhuzhou City, Hunan Province, PRC, 412000). SEM images of the top surfaces of the NMC and graphite electrodes are presented in Figure S1 so that readers can appreciate the morphology of the particles that make up the electrodes. Before electrolyte filling, the pouch cells were cut just below the heat seal and dried at 80°C under vacuum for 12 h to remove any residual water. Cells were then filled with 0.9 g of electrolyte in an argon-filled glove box. In this study, 1 M LiPF_6 (BASF, purity 99.94%, water content 14 ppm) EC:EMC (3:7 by weight, BASF, water content less than 20 ppm) was used as the control electrolyte. To this electrolyte, 2 wt% of VC (BASF, purity > 99.8%, water content < 100 ppm) was added singly or in combination with 2 wt% ES (Aldrich, purity > 99.0%). The cells were then vacuum-sealed at a gauge pressure of -94 kPa (relative to atmospheric pressure) using a compact vacuum sealer (MSK-115A, MTI Corp.). For each of the following formation/cycling/storage experiments, two identical pouch cells were prepared for each electrolyte blend to confirm the reproducibility of the corresponding electrochemical tests.

Cell formation, cycling and storage protocol. After filling, formation was performed on a Maccor 4000 series cycler as follows. Cells were placed in a temperature-controlled box at $40. \pm 0.1^\circ\text{C}$ and held at 1.5 V for 24 h to allow for the completion of wetting. Cells were then charged to 3.8 V using a current of 11 mA (C/20). After this step, cells were cut open in an argon-filled glove box to release any gas generated during formation and then vacuum sealed again. Cells were then charged to 4.2 V and discharged to 2.8 V at 11 mA (C/20). Note that for each charge/discharge step during formation, pouch cells intended for the XPS study were held at the chosen voltage until the measured current decreased to 0.005C so that electrodes were in electrochemical equilibrium.

For the XPS study, cells were cycled on a Maccor 4000 series cycler between 4.2 and 2.8 V at $40. \pm 0.1^\circ\text{C}$ and 11 mA (C/20) for 24 cycles (*i.e.* 25 cycles including the formation cycle) then cells were stopped either fully charged at 4.2 V or fully discharged at 2.8 V. Pouch cells were then carefully disassembled in an argon-filled glove box within the 24 h following the end of the formation/cycling processes. Negative graphite and positive NMC electrodes were cut from the pouch cells electrodes with a precision punch and washed twice by immersion into 0.8 mL of EMC solvent (BASF) in a clean and dry glass vial with a mild manual agitation for 10 s to remove the majority of the LiPF₆ salt. Electrodes were then dried at approx. 10⁻³ mbar in the antechamber of the glove box overnight then stored in sealed glass vials in the argon-filled glove box prior to the XPS analysis.

For the dQ/dV vs. V analysis, the graphite potential was estimated as follows: High-precision reference potential-specific capacity data for Li/graphite and Li/LiNi_{1/3}Mn_{1/3}Co_{1/3}O₂ electrodes

as well as the full $\text{LiNi}_{1/3}\text{Mn}_{1/3}\text{Co}_{1/3}\text{O}_2$ /graphite pouch cell voltage-specific capacity data were first recorded. Then, from these data, the dV/dQ vs. Q of a $\text{LiNi}_{1/3}\text{Mn}_{1/3}\text{Co}_{1/3}\text{O}_2$ /graphite pouch cell is calculated and compared to the experimental curve using a differential potential analysis software previously developed at Dalhousie University⁴³. Using this method, no reference electrode is needed to obtain the anode potential versus lithium metal.

The Ultra High Precision Charger (UHPC) built at Dalhousie University^{41,42} was used to monitor the coulombic inefficiency and charge end point capacity slippage⁴⁴ of NMC/graphite pouch cells between 2.8 and 4.2 V at $40. \pm 0.1^\circ\text{C}$ using a current of 11 mA (C/20) for 15 cycles where comparisons were made. Note that the accuracy of the UHPC system has been shown to be about two orders of magnitude better than that of high-end commercial charger systems⁴². The CIE was calculated from the CE taken as an average of the final three data points (cycles 13–15) collected on the UHPC. The charge end point capacity slippage rate was calculated from the slope of a best fit line to the final five points (cycles 11–15) of the charge end point capacity versus cycle number curve.

For storage, cells were first charged with a Maccor series 4000 cycler to 4.2 V using a current of 11 mA (C/20) then held at 4.2 V until the measured current decreased to 0.0025C. After the pre-cycling process, cells were carefully moved to the storage system which automatically monitored their open circuit voltage every 6 hours for a total storage time of 500 h.⁴⁵

Additional long term cycling was also performed in order to evaluate the expected cycle life. For this purpose, NMC/graphite pouch cells were cycled on a Neware BTS3000 system between 2.8 and 4.2 V at 220 mA (C) and at $40. \pm 0.1^{\circ}\text{C}$.

Gas measurements. The volume of gas generated during formation, storage and cycling was measured using Archimedes' principle by weighing cells before and after testing. For *ex-situ* gas volume measurements, pouch cells were suspended from a fine wire "hook" attached under a Shimadzu balance (AUW200D). Pouch cells were then immersed in a beaker of de-ionized "nanopure" water ($18 \text{ M}\Omega\text{.cm}$) at $20 \pm 1^{\circ}\text{C}$. Before weighing, all cells were charged or discharged to 3.80 V. For *in-situ* gas volume measurements, the Archimedes in situ gas analyzer (AISGA) recently developed at Dalhousie University and fully described in reference ⁴⁶ was used to accurately measure gas evolution during the early stage of the formation cycle. A strain gauge load cell was used to measure changes in the buoyant force of pouch cells submerged in silicone oil kept at $40. \pm 0.1^{\circ}\text{C}$ by a temperature-controlled box. The random error in the strain gauge measurements, due to the resolution, has been measured to be 0.01 mL. However, from duplicate measurements of pouch cell gas evolution, the systematic error was estimated to be about 0.1 mL.

Gas chromatography coupled with electron impact mass spectroscopy (GC-MS).

Liquid electrolyte analysis - The procedure for the extraction of electrolyte components for GC-MS analysis followed the one previously described by Petibon *et al.*⁴⁴. This simple method allows salts such as LiPF₆, which might damage the GC column, to be removed. Prior to GC-MS

analysis, pouch cells were first discharged to an open circuit voltage near 0.0 V and opened rapidly outside the glove box. The jelly roll was then immediately put in a perfluoroalkoxy polymer (PFA) vial containing 10 mL of dichloromethane (DCM). The vial was then shaken automatically for 15–20 min to extract the electrolyte from the jelly roll. The supernatant was then filtered using a syringe filter with a PTFE membrane and 0.2–0.45 μm pores. A few drops of the filtrate were then added to a vial containing 10 mL of DCM and 0.25 mL of distilled water, shaken for 5–10 min and centrifuged at 300 g-force for 10–15 min to eliminate any potential emulsion. The organic layer (the lower layer) was then injected in the GC-MS. The exact volume and weight of filtrate added were not measured. During short term cycling at ambient temperature (less than a year) and modest voltages, the amount of EC consumed is expected to be small. During each GC-MS measurement, EC, EMC, the additive studied, along with known trans-esterification products of EMC and EC were quantified. As the exact volume (or weight) of the filtrate is not known, the quantification gives a relative mass percent of each compound quantified. The results presented in this report are then weight percent of the additive relative to the total mass of EC, EMC, known trans-esterification products of EMC or EC and the additive.⁴⁴

The GC-MS used was a Bruker 436-GC equipped with a split/split-less injector and a BR-5MS 30 m column with an inner diameter of 0.25 mm and a coating thickness of 1 μm . Helium was used as carrier gas at a constant flow rate of 1.3 mL/min. The GC was coupled to a Bruker Scion single-quadrupole mass spectrometer equipped with an electron impact ionization module. The injector temperature was set to 270°C and the oven temperature was programmed to get the best component separation in the shortest amount of time. The end of the oven temperature cycle was

set to 290°C for 5 min to ensure the elution of heavier highly retained compounds (mostly compounds coming from septum and column bleed). The transfer line was set to 270°C, the ion source to 270°C and the electron energy to 70 eV. The mass spectrometer was set to a single ion monitoring mode (SIM) for the measurement of EC, EMC, DMC, DEC, VC, ES and known addition products of EC with either EMC, DMC, or DEC, DMC, DEC. The addition products were monitored in the eventuality that they would form during formation. After the SIM mode measurements, all solutions were measured again with the MS set to a full scan mode to verify that no other compound was present. For quantitative analysis of electrolyte components, calibration solutions (five minimum) were made by diluting known amounts of electrolyte solvents and additives in DCM to obtain an external calibration curve with a squared correlation coefficient of at least 0.999.

The detection limit of the single ion GC-MS used in this study is about 100 ppb and the error for an individual measurement was estimated to be less than 3%. The results presented here are the average from measurements made on a minimum of two identical pouch cells.

Gas analysis - GC-MS was also used to analyze the different gases formed other than H₂ during cell use with different electrolyte blends. After formation at 2.4 V or 3.5 V (at 11 mA, C/20 and 40. ± 0.1°C), cells were immediately removed from the temperature box, discharged to 0 V and put in a brass chamber as shown in Figure S2. The chamber was fitted with a Swagelock quick-connect on one end, and a septum on the other end. The cap of the chamber was fitted with a

shaft, having a sharp point, allowing the pouch cell bag to be punctured. The shaft was fitted with two o-rings to prevent gas exchange between the exterior and the interior of the chamber.

The brass chamber with the cell fitted inside was pumped down to a pressure of 100 mTorr. The shaft was lowered to puncture the bag of the pouch cell. The low pressure in the chamber forces the gas out of the pouch cell inside the chamber, along with any high vapor pressure compounds potentially formed during the pouch cell formation. The chamber was then back-filled with argon to equilibrate the pressure inside and outside the chamber. The gas from the chamber was then extracted from the chamber using a gas tight syringe.

The extracted gas was then injected in the GC-MS. The column used for gas analysis was a Bruker Q-PLOT 30 m column with an inner diameter of 0.25 mm and a divinylbenzene polymer coating thickness of 8 μm . Helium was used as carrier gas at a constant flow rate of 1.3 mL/min. The injector temperature was set to 100°C and the oven temperature was programmed to get the best component separation in the shortest amount of time. The end of the oven temperature ramp, transfer line temperature, source temperature and electron energy were kept the same as for the solvent analysis of the electrolyte.

The particular setup did not allow H₂ to be detected (spectrometer limitation) and did not allow O₂, N₂ or CO to be separated (column limitation). For this reason, the mass spectrometer was set to a single ion monitoring mode for the ion fragments 32 (O₂), 28 (N₂ and CO) and 12 (carbon

from CO) in the time range where these gases eluted from the column. Since CO and N₂ possess the same principal ion fragment (28), CO was detected using the fragment m/z = 12 (5% of the intensity of the fragment m/z = 28). The mass spectrometer was set to a full scan for the detection of the other gases. The gas sample transfer method allows some ambient air to enter the syringe needle. As a consequence, the O₂ and N₂ detected during analysis were ignored. This is not troublesome since O₂ is unlikely to be generated during the early first charge of the pouch cells and since no nitrogen-containing components or chemicals are present in the cell.

X-ray Photoelectron Spectroscopy (XPS). XPS was performed on a SPECS spectrometer equipped with a Phoibos 150 hemispherical energy analyzer and using Mg K α radiation ($h\nu = 1253.6$ eV). To transfer air sensitive samples from the argon-filled glove box to the spectrometer, a special transfer system (Figure S3) fully described in reference 24 was used. Shortly, samples were mounted onto a molybdenum holder using a copper conductive tape (3M) and placed into the transfer system in an argon-filled glove box. The latter was then put under vacuum at a pressure of approx. 10⁻³ mbar during 1 h before to be connected to the spectrometer where the samples were loaded under a pressure of ~10⁻³ mbar. All samples were kept under a pressure of 10⁻⁸ mbar overnight before analysis to allow a strictly identical vacuum procedure.

Sample analysis using XPS was performed as follows. The analyzed sample area was ~ 2 x 3 mm² which gives results representative of the whole electrode. Core spectra were recorded in the fixed analyser transmission (FAT) mode with a pass energy of 20 eV at an operating pressure lower than 2 x 10⁻⁹ mbar. Short acquisition time spectra were recorded first as a reference to

follow any possible sample degradation during the analysis. CasaXPS software was used for the data treatment. The binding energy scale was calibrated from the C1s peak at 285 eV (C-C/C-H) and the O1s peak at 529.6 eV (O^{2-} anion from the $LiNi_{1/3}Mn_{1/3}Co_{1/3}O_2$ active material) for negative graphite and positive NMC electrodes respectively. Core peak analysis was performed using a nonlinear Shirley-type background.⁴⁵ The peak positions and areas were optimized using 70% Gaussian - 30% Lorentzian Voigt peak shapes and full width at half-maximum (fwhm) constraint ranges. The following fitting procedure was then followed. A minimum number of peaks were used for the core level spectra of electrodes taken from the control cells (with no additives). When additives were used, an equal number of peaks was chosen as a first assumption and peak positions were fixed using a position constraint of ± 0.2 eV. Then, based on the residual spectra as well as the difference spectra, additional peaks were added when clearly necessary. If additional peak(s) were needed, the position constraint was then modified to ± 0.5 eV to allow a more accurate fitting. In that case, if a significant peak shift (≥ 0.3 eV) was observed, this peak shift was considered as reliable and, therefore kept only if an identical peak shift was also observed for each other electrode samples for a given additive blend. In the different Figures, core level spectra of graphite electrodes were maximized to show low intensity peaks, while core level spectra of NMC electrodes were normalized to show the same intensity range. The reproducibility of XPS spectra and quantification was confirmed on 6 sets of pair pouch cells over 24 different sets analyzed in total in the present study.

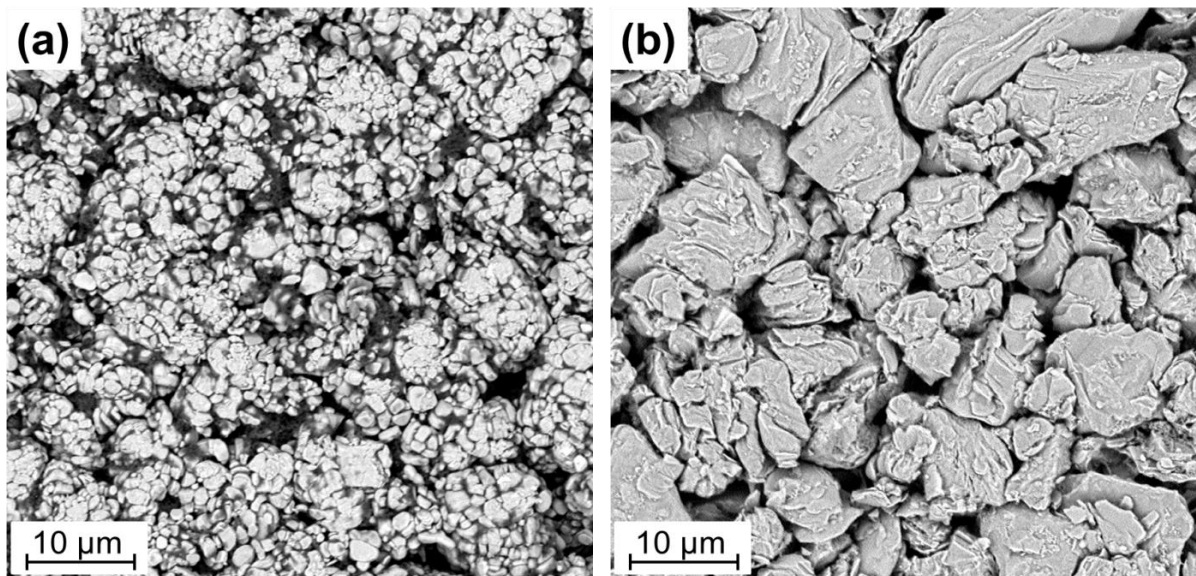


Figure S1. SEM images of the top surface of (a) the NMC electrode and (b) the graphite electrode taken from a dry pouch cell.

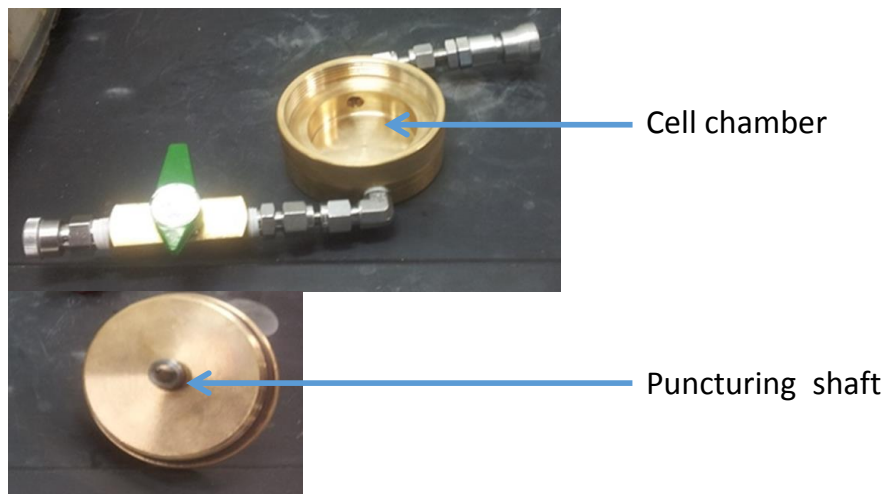


Figure S2. Picture of the gas extraction device designed for the extraction of gaseous and volatile components of Li-ion pouch cells. Designed with the help of Simon Trussler, Physics & Atmospheric Science, Dalhousie University (2014).

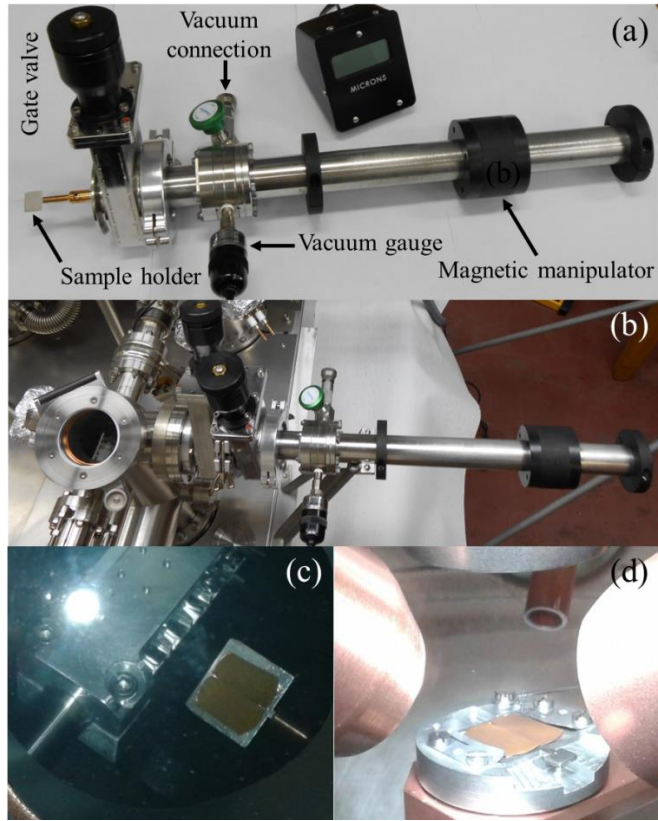


Figure S3. (a) Transfer system used at Dalhousie University. It is composed of a magnetic manipulator attached to a sample holder, a gate valve and a flange that fits the entry port of the spectrometer. It can therefore be placed under vacuum via a needle valve while the vacuum level can be monitored by a vacuum gauge. Note that no significant pressure change was observed when the transfer system was left without sample under static vacuum at $\sim 10^{-3}$ mbar for 1 night demonstrating that the transfer system was leak free; (b) a photograph of the transfer system when connected to the XPS system; (c) and (d) photographs of two lithiated graphite electrodes from two different pouch cells charged at 4.2 V and loaded into the load lock and the analysis chamber of the XPS spectrometer, respectively. Photos were taken through glass viewports. The gold color that corresponds to the fully lithiated state of the graphite demonstrates the reliability of the electrode sample preparation and transfer protocol. Please note that lithiated graphite samples exposed to the humid air of our laboratory lose their gold color within a few seconds.

Table S1. Capacity associated (mAh) with the 24 h hold step at 1.5 V during the formation process of the NMC/graphite pouch cells for the different electrolyte blends. The capacities varied by ± 0.1 mAh between pair cells.

Electrolyte blend	Control	2% VC	2% ES	2% VC + 2% ES
24 h hold capacity (mAh)	0.4	0.55	1.7	0.7

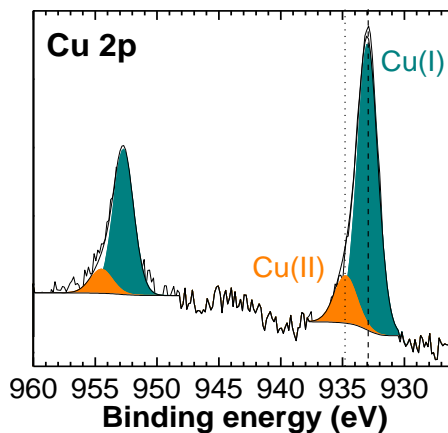


Figure S4. Cu 2p XPS core spectrum of the graphite electrode after formation at 2.4 V and 40°C with 2% ES electrolyte. The two Cu 2p components can be attributed to Cu(I) from Cu₂O and Cu(II) from CuO.⁵¹

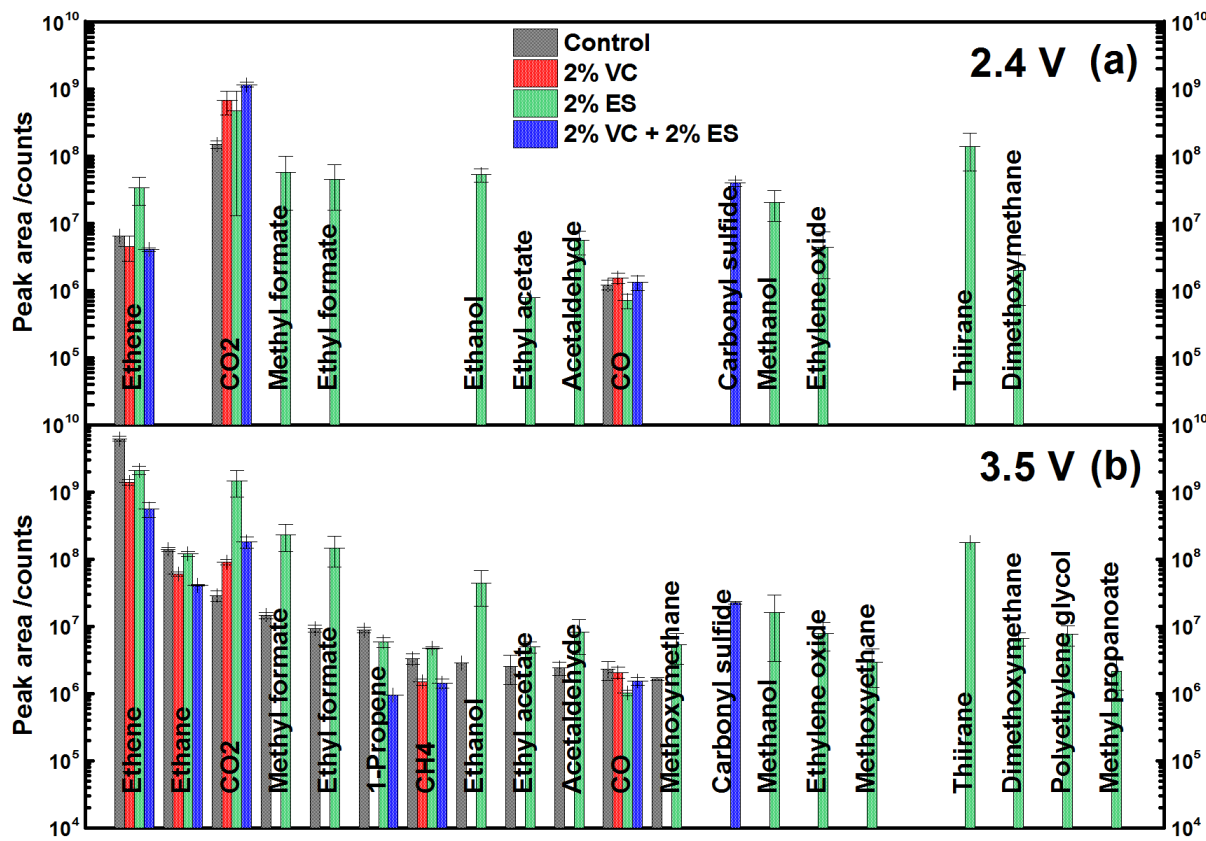


Figure S5. Complete GC-MS data for gases extracted from NMC/graphite pouch cells for the different electrolyte blends after formation at (a) 2.4 V and (b) 3.5 V. The data presented here shows the normalized peak area for compounds that are gaseous at room temperature

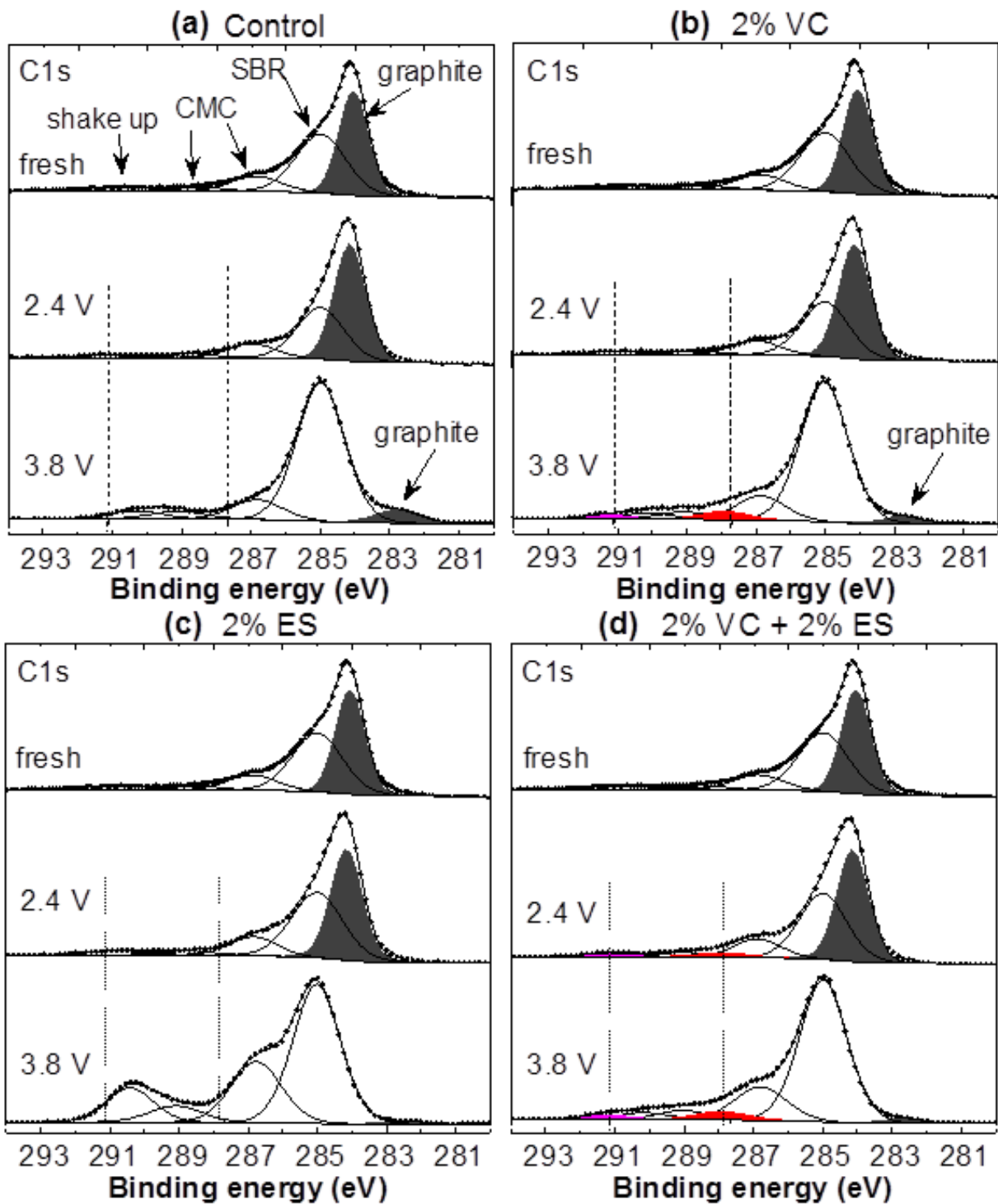


Figure S6. Enlarged C 1s XPS core spectra for graphite electrodes with (a) control, (b) 2% VC, (c) 2% ES, and (d) 2% VC + 2% ES electrolytes taken from cells during formation at 2.4 V, 3.8 V during charge at C/20 and $40. \pm 0.1^\circ\text{C}$ compared to the fresh electrode.

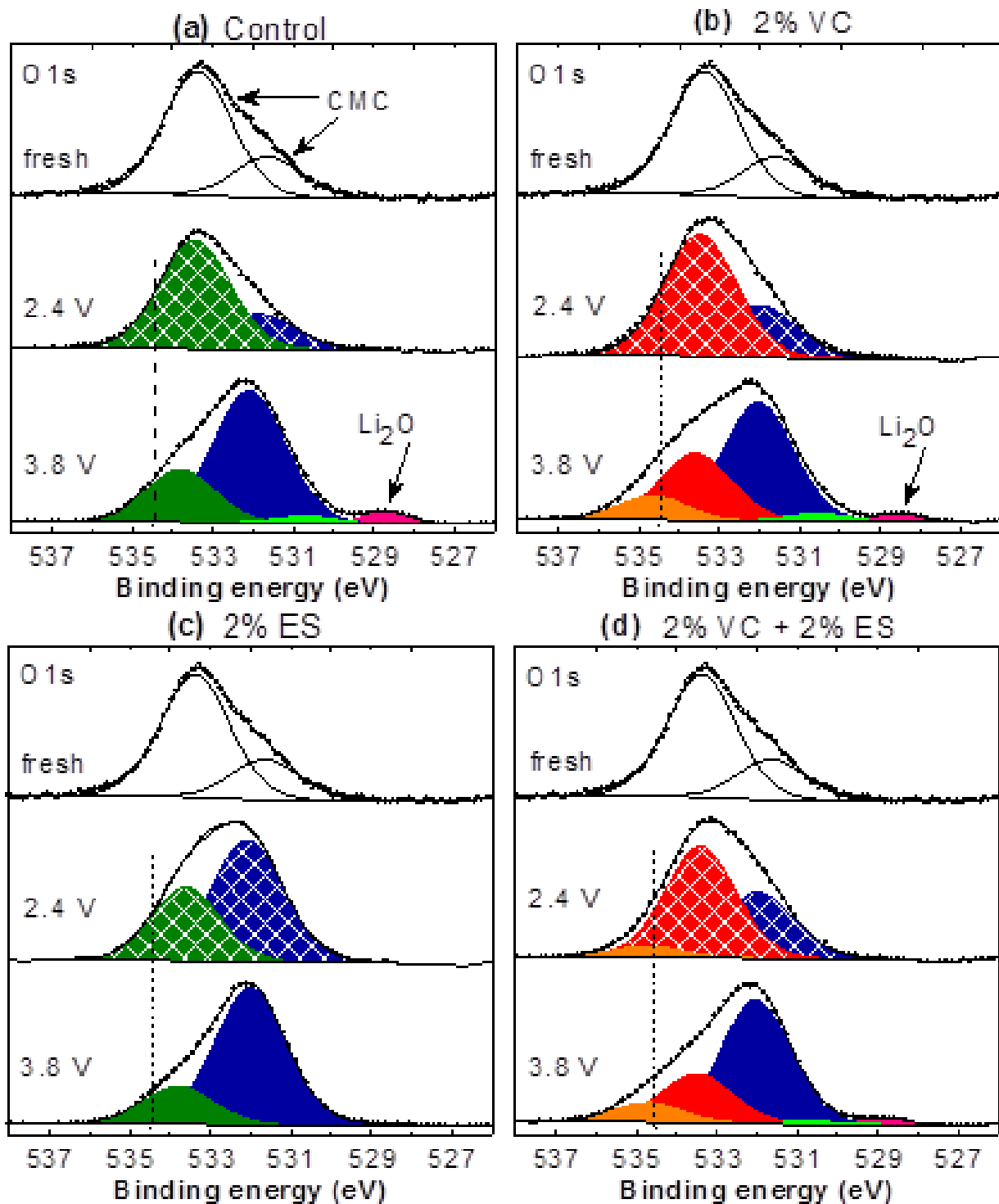


Figure S7. Enlarged O 1s XPS core spectra for graphite electrodes with (a) control, (b) 2% VC, (c) 2% ES, and (d) 2% VC + 2% ES electrolytes taken from cells during formation at 2.4 V, 3.8 V during charge at C/20 and $40. \pm 0.1^\circ\text{C}$ compared to the fresh electrode.

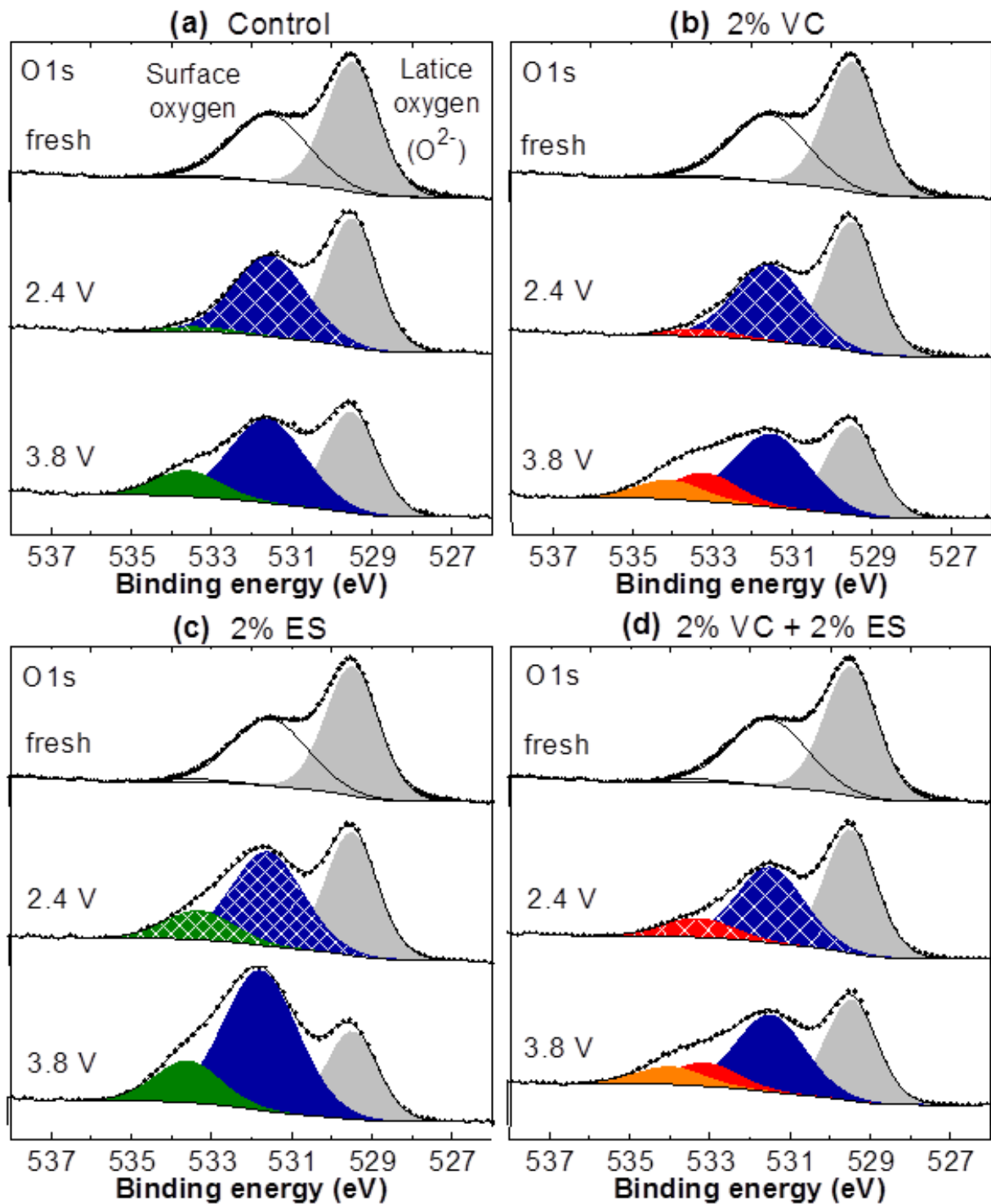


Figure S8. Enlarged O 1s XPS core spectra for NMC electrodes with (a) control, (b) 2% VC, (c) 2% ES, and (d) 2% VC + 2% ES electrolytes taken from cells during formation at 2.4 V, 3.8 V during charge at C/20 and $40. \pm 0.1^\circ\text{C}$ compared to the fresh electrode.

Table S2. Atomic percentage (at. %) of the P 2p peaks associated with phosphates (P_xO_y) and fluorophosphates ($Li_xPO_yF_z$) as measured from the XPS quantification at the graphite surface as function of the voltage of the cell during formation and after cycling.

Sample	P_xO_y						$Li_xPO_yF_z$					
	2.4V	3.8V	4.2V	2.8V	C4.2	D2.8	2.4V	3.8V	4.2V	2.8V	C4.2	D2.8
Control	0	0.5	1.8	0.3	1.9	1.0	< 0.1	0.4	0.8	0.4	0.8	0.7
2% VC	0	0.4	0.3	0.4	1.3	0.6	< 0.1	0.3	0.4	0.6	1.3	0.6
2% ES	< 0.1	0.5	0.3	0.2	1.1	0.5	0.1	0.2	0.2	0.4	0.5	0.3
2% VC + 2% ES	0	0.7	0.2	0.1	0.9	0.5	< 0.1	0.2	0.4	0.1	0.8	0.5

Table S3. Atomic percentage (at. %) of the P 2p peaks associated with phosphates (P_xO_y) and fluorophosphates ($Li_xPO_yF_z$) as measured from the XPS quantification at the NMC surface as function of the voltage of the cell during formation and after cycling.

Sample	P_xO_y						$Li_xPO_yF_z$					
	2.4V	3.8V	4.2V	2.8V	C4.2	D2.8	2.4V	3.8V	4.2V	2.8V	C4.2	D2.8
Control	0	0.1	0.2	0.2	0.4	0.3	0.4	0.1	0.3	0.2	0.3	0.4
2% VC	0.2	0.1	0.1	0.2	0.3	0.3	0.2	0.2	0.5	0.3	0.2	0.3
2% ES	0.2	0.2	0.2	0.1	0.3	0.3	0.4	0.6	0.5	0.4	0.3	0.4
2% VC + 2% ES	0.1	0.1	0.2	0.1	0.3	0.2	0.3	0.2	0.7	0.4	0.5	1.1